Mechanical Systems and Signal Processing, Volume 25, Issue 1, January 2011, Pages 266–284

The application of spectral kurtosis on Acoustic Emission and Vibrations from a defective bearing

B Eftekharnejad, M R Carrasco, B Charnley and D Mba

School of Engineering, Cranfield University, Bedford, United Kingdom MK43 0AL

Tel: +44 (0) 1234 750111 ext 4786

Fax: +44 (0) 1234 751566

Email: d.mba@cranfield.ac.uk

Abstract

The application of Acoustic Emission (AE) technology for machine health monitoring is gaining ground as power tool for health diagnostic of rolling element bearing. This paper provides an investigation which compares the applicability of AE and vibration technologies in monitoring a naturally degraded roller bearing. This research is first known attempt investigating the comparative effectiveness of applying the Kurtogram to both vibration and AE data from a defective bearing.

Keywords: Acoustic Emission, Condition monitoring, Spectral Kurtosis, Vibration, Kurtogram

1. Introduction

The rolling element bearing is the most common part of any rotating machine and monitoring its integrity is of vital importance. Vibration monitoring is the most widely used method for bearing diagnosis where signals are normally processed in time or frequency domains. In the time domain, typical statistical features of the measured vibration signal such as r.m.s, peak value and Kurtosis, etc, are trended over the duration of the test and changes in patterns are attributed to presence of defects. Among these statistical features, the value of Kurtosis was found to be most effective in detecting the onset of bearing failure [1] .For an undamaged bearing the Kurtosis is typically 3 while greater values are normally associated with loss of integrity. However, the main drawback of using this method is that the Kurtosis begins to revert

back to the undamaged value as the defect further develops [1, 2]. Other statistical features such as the Kolmogorov – Smirnov statistic has been applied by several investigators [3, 4] in which they reported success in diagnosing a damaged bearing. Frequency domain analysis for machine fault diagnosis is well established and the authors refer the readers to a review by Patil et al[2].

The application of Acoustic Emission (AE) in monitoring the rolling element bearings has grown in popularity over the past few decades [5]. To date most of the published works have studied the applicability of AE technology in detecting seeded faults artificially introduced on the bearing. Yoshioka[6] was among the first who studied the applicability of AE in detecting naturally degraded roller bearing. However, the number of rollers employed in Yoshioka's research was limited to three which is not representative of operational bearings. Additionally, Yoshioaka terminated the test once the AE level reached to a certain predefined threshold therefore propagation of the surface defect was not monitored. Later, Elforjani et al [7, 8] conducted an experiment which built on Yoshioka's work. Their results showed the effectiveness of AE in detecting the onset of bearing failure, identifying the circumferential location of the defect on the race at very early stages of degradation, and the diagnostic potential of the measured AE signal by enveloping and using the KS statistic. Although conclusive, this research was not representative of broad operation condition as the test was at a slow rotational speed (72 r.p.m). The results presented in this paper aim to compliment the work of Elforjani [7, 8] by experimentally investigating the use of AE for detecting natural degradation of a bearing at a rotational speed of 1500 r.p.m. In addition, the use of the Kurtogram for improving signal-to-noise ratios on AE waveforms from a bearing is explored.

The Spectral Kurtosis (SK) as an effective signal processing method is gaining ground in vibration analysis. To determine the SK the signal is firstly decomposed into the time-frequency domain after which the Kurtosis values are determined for each frequency band [9]. The concept of SK analysis was first developed by Dwyer [10] as a tool which was able to trace non-Gaussian features in different frequency bands using the fourth order moment of the real part of the Short Time Fourier Transform (STFT). Dwyer only investigated the application of SK on stationary processes but did not account for non-stationary vibration signatures typical of rotating machines.

To date the most comprehensive calculations of the SK has been developed by Antoni [11] as the fourth order cumulant of the spectral moment *(K)* :

$$K_Y(f) = \frac{S_{4Y}(f)}{S_{2Y}^2(f)} - 2 \quad f \neq 0 \qquad (1)$$

and

$$S_{nY}(f) \overset{\Delta}{=} \langle |Y_W(t, f)|^n \rangle \qquad (2)$$

$Y_W(t, f)$ is estimated using the short time Fourier Transform:

$$Y_W(t, f) \overset{\Delta}{=} \sum_{-\infty}^{\infty} Y(n) \cdot W(n - t) e^{-j2\pi nf} \qquad (3)$$

Where *Y(n)* is sampled version of the signal, *Y(t)*, and *W(n)* is the window function having zero value outside a chosen interval. For the above calculations to be valid the size of window (*Nw*) should smaller than the length between two repetitive impulses and longer than length of each impulses. In other word, the analyzed signal should be locally stationary. Using the definition offered by Antoni [11], Antoni and Randall [12] developed the concept of the Kurtogram to detect non-guassinatiy in a signal. A Kurtogram simply maps the STFT-based SK values as function of frequency and window size. Antoni [11, 12] suggested the use of the Kurtogram for designing a band-pass filter which can be applied to increase the signal–to-noise ratio thereby preserving the impulse-like nature of signal. For this particular investigation the frequency and window size (bandwidth) at which the Kurtogram is maximum was employed to build a band-pass filter which was applied to measured AE and vibration data. This research is first known attempt investigating the comparative effectiveness of applying the Kurtogram to both vibration and AE data from a defective bearing.

2. Experimental Setup

The test rig used in this experiment was of the same arrangement as employed by Elforjani et al [8], see figure 1. It consisted of a hydraulic loading device, a geared electrical motor (MOTOVARIO-TypeHA52 B3-B6-B7 j20, 46-Lubricated: AGIP), a coupling and a supporting structure. The bearing test rig has been designed to simulate varying operating conditions for a bearing and fail this bearing in fatigue.

The chosen bearing for this study is an SKF single thrust ball bearing, model number SKF51210. This bearing was chosen as it was easily available and cost effective to use. To ensure fatigue cracking initiation in the ball race being monitored the standard grooved race was replaced with a flat race, model number SKF 81210TN. This increased the point contact force between the ball bearings and the race resulting in faster degradation of the bearing race and early initiation of sub surface fatigue cracks. For the purpose of this experiment the following procedure was undertaken to determine the subsurface stresses on the test bearing and thereby estimate the time, or number of cycles, prior to a surface defect on the race track. Theories employed for this procedure, particularly for the flat race, included the Hertzian theory for determining surface stresses and deformations, the Thomas and Hoersh theory for subsurface stress, and the Lundberg and Palmgren theory for fatigue evaluation. For the grooved race the standard procedure, as described by BS 5512,1991, was employed for determining dynamic load rating .Theoretically determined life was calculated to be 16 t hours.The test bearing was placed between the fixed thrust loading shaft and the rotating disk which housed the grooved race. The flat race was fitted onto the loading shaft in a specifically designed housing. This housing was constructed to allow for placement of AE sensors directly onto the race. The thrust shaft was driven by a hydraulic cylinder (Hi-Force Hydraulics-Model No: HP110-Hand Pump-Single Speed-Working Pressure: 700 bar), which moved forward to load the bearing and backwards for periodic inspections of the test bearing face. The rotating disk was driven by a shaft attached to a motor with an output speed of 1500 rpm. The number of rolling elements used in this research was 14 and the ball pass frequency (BPF) was calculated as 175Hz using equation 4 [1] .

$$BPF = \frac{1}{120} nN\left(1 - \frac{d}{D}\cos\alpha\right) \qquad (4)$$

Where,

d=Ball diameter

D=Pitch diameter

α=Contact angle

n=Shaft rotation velocity (RPM) N=Number of balls

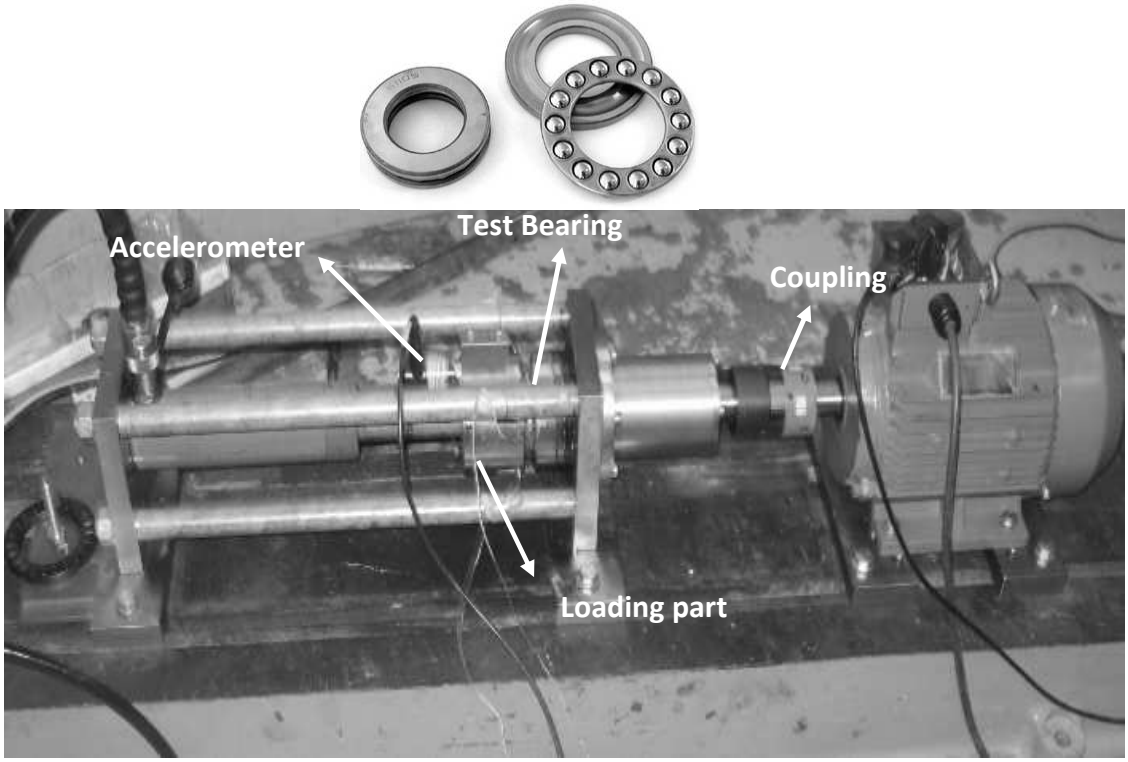

Figure 1 The test rig assembly

The AE acquisition system employed commercially available piezoelectric sensors (Physical Acoustic Corporation) with an operating range of 100–750 kHz. All four AE sensors were mounted at the back of the flat race test bearing and connected to a data acquisition system through a preamplifier (40 dB gain) AE waveforms were taken every three minutes throughout the test duration at the sampling rate of 2 MHz.

An accelerometer was mounted on the flat race housing (see figure 1) and vibration measurements were acquired at a sampling rate of 10 kHz at three-minute intervals using a NI-6009 USB analog to digital data acquisition card.

3. Test procedure

The test rig was allowed to operate until vibration levels far exceeded typical operating levels at which point the test was terminated. An axial load of approximately 50000N was applied on the bearing throughout the test and a total of three tests were performed.

Two tests are presented in this paper with quite distinct signal-to-noise ratios; Test 2 was significantly nosier for both vibration and AE measurements. This was attributed to the variation in test rig assembly, such as adjustments and sensor attachments therefore it offered a good opportunity to asses methods for diagnosis.Such challenges with AE sensor attachment and noise interference have been discussed recently [13]. The overall trends of Acoustic Emission and vibration levels for both tests are presented in figure 2. Also presented in figure 3 is the defect observed on termination of Test-1 clearly displaying a spall on the flat race.

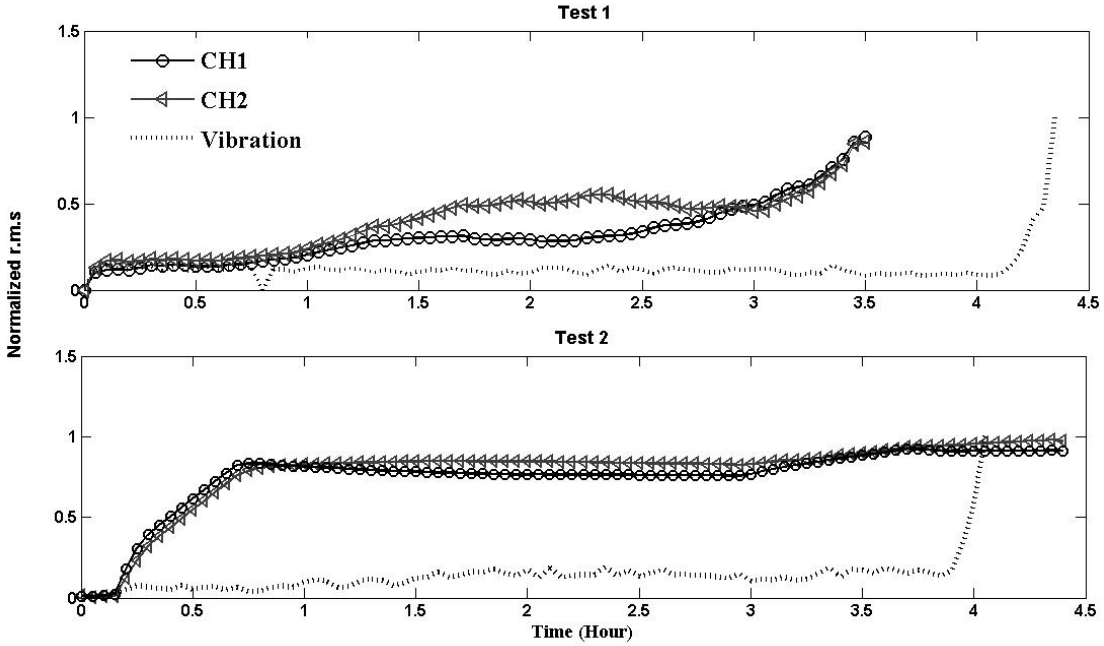

Figure 2 Overall AE and vibration r.m.s levels

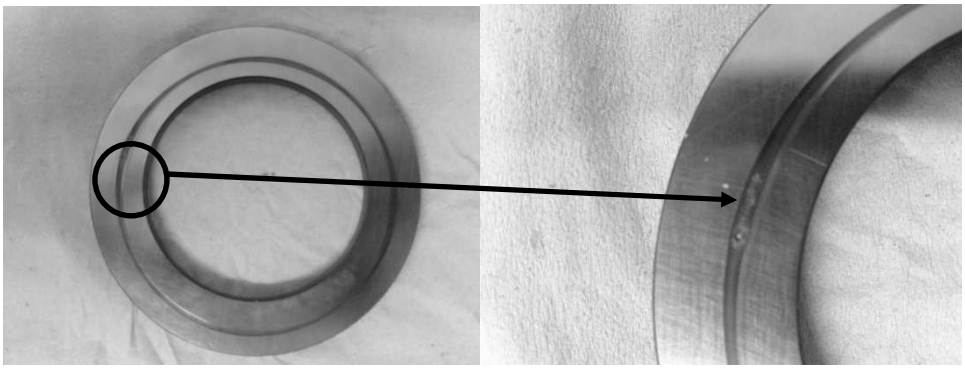

Figure 3 Defect on the outer race (naturally developed over 4hrs of operation)

4. Vibration Monitoring

The vibration waveforms for both tests at defined time intervals are detailed in table 1 and figure 4.Under ideal conditions it would be expected that for the particular type of defect generated during the test (see figure 3) large transient vibration impulses spaced at defect frequency would be evident. This defect frequency is characteristic of the bearing elements. However, due to the high level of operational noise, resulting in a low signal to noise ratio, the presence of these spikes was not always visually evident in the captured waveforms. The frequency spectrums of the waveforms are also presented in figure 5. The Ball Pass Frequency (BPF) was evident at stages 'E' and 'F' of Test-1 whilst this defect frequency was barely present at stages 'E' and 'F' on Test- 2. In addition several harmonics of the running speed (25 Hz) was noted with the third harmonic (75 Hz) dominant for both tests. In an attempt to achieve a better resolution in detecting the fault frequency envelope analysis was undertaken. The signals were band pass filtered about a centre frequency of 1570 Hz using the least-square FIR filter of order 50 with a bandwidth of 40Hz . Selection of this centre frequency was based on observation of the spectrum of the last recorded vibration stage where a large peak was evident at 1570 Hz for both tests, see figure 6. It is believed that this frequency (1570 Hz) is associated with one of the resonance frequencies of the bearing test-rig and this frequency was excited due to the impulsive impacts of the rollers over the defective race. The filtered signals were enveloped

using the Hilbert transform. Figure 7 presents the envelope spectrum of the filtered signals with the defect frequency now clearly evident at interval 'F' particularly for test 2. This was to be expected given the selected frequency for filtering was chosen from the spectrum at interval 'F'. This also shows that the selection of the filtering frequency is dependent on the dynamic characteristic of the bearing/machine at the time of vibration measurement as seen in figure 6 where the filtering frequency of 1570 Hz was not dominate at the earlier test intervals.

Table 1 Timing interval

	Test 1	**Test 2**
A	40 min	40 min
B	80 min	80 min
C	120 min	120 min
D	180 min	160 min
E	220 min	200 min
F	264 min	240 min

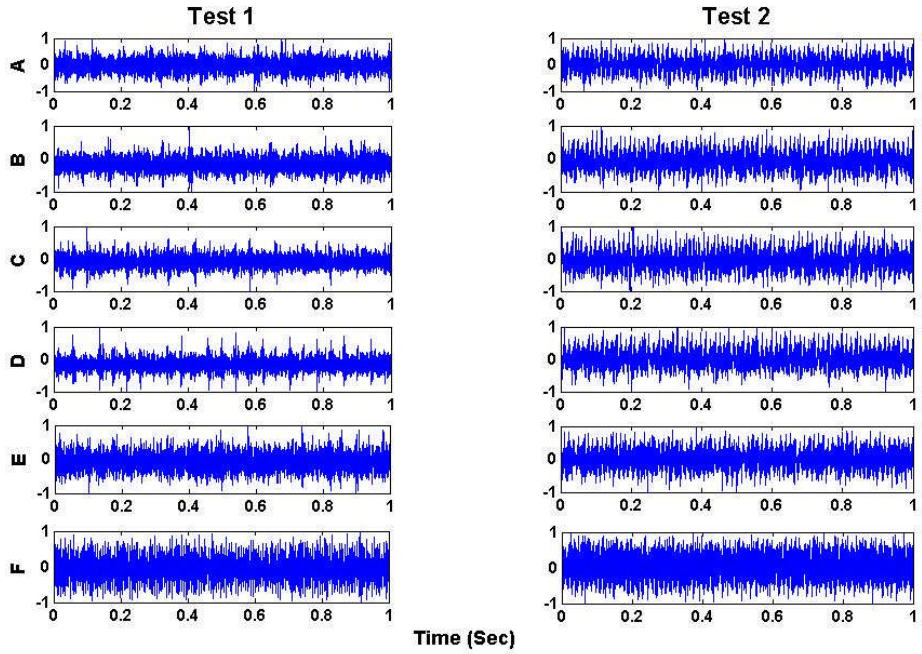

Figure 4 The vibration waveform associated with different test intervals.

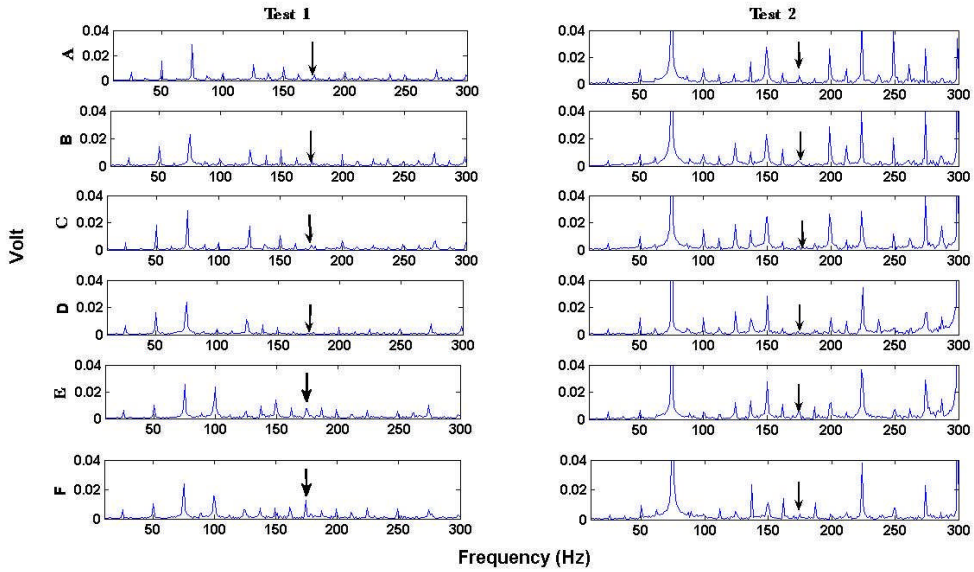

Figure 5 FFT of the signals at different interval [10Hz-300Hz]

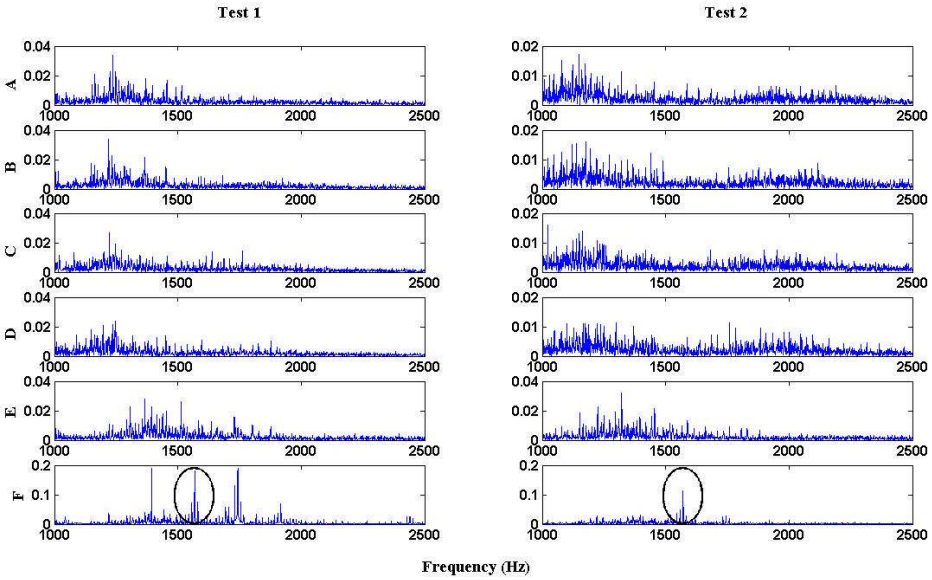

Figure 6 Vibration frequency spectrum

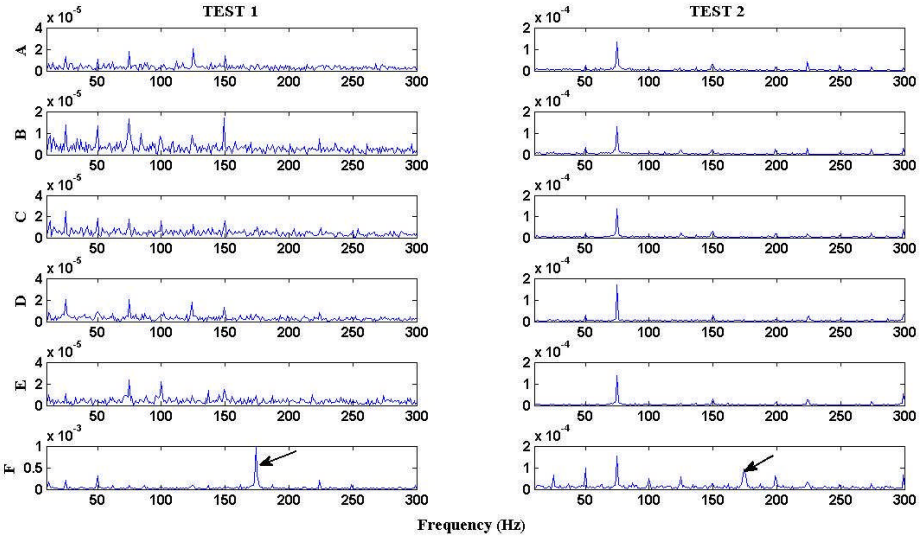

Figure 7 The envelop spectrum of the Vibration signals filtered at 1570 Hz

Although performing envelop analysis in conjunction with band-pass filtering was successful in discriminating the BPF, prior knowledge of entire frequency spectrum and location of dominant amplitude across the spectrum is essential for selection of the most effective filter frequency. Furthermore, since the presence of random Gaussian noise can affect the resolution of frequency spectrum, and this can vary at the different stages of mechanical integrity, the estimation of the optimum filter frequency can be challenging. This is very important when dealing with the intelligent monitoring systems, in which automatic selection of filter frequencies can be significantly influenced by the level of signal-to-noise ratio. Indeed, the key to performing an effective envelop analysis is to choose an effective band-pass filter and since the rolling bearings in practice are operated under different working conditions (speed and load), a generic band-pass filter with fixed parameters (Centre frequency and Band width) will not be sensitive enough to perform a compelling diagnosis [14]. One such method for optimal filter selection is the spectral Kurtogram.

In order to improve the denoising of vibration signals the concept of Spectral Kurtosis (SK) was employed. This involves calculating the Kurtogram for each signal from which the bandwidth and centre frequency required to design a band-pass filter are determined. The criterion was set such that the frequency and bandwidth (Window size) at which the spectral kurtosis of the signal is maximum was employed to build a new band pass filter. The determination of SK was based on the algorithm developed

by Antoni [15, 16]. A sample Kurtogram of signals at an early stage (A) and upon the termination (F) of tests are presented in figure 8. The centre frequency (Fc) at 'F' was significantly higher than at interval 'A' suggesting a change in the impulsive vibration nature as the defect matured.

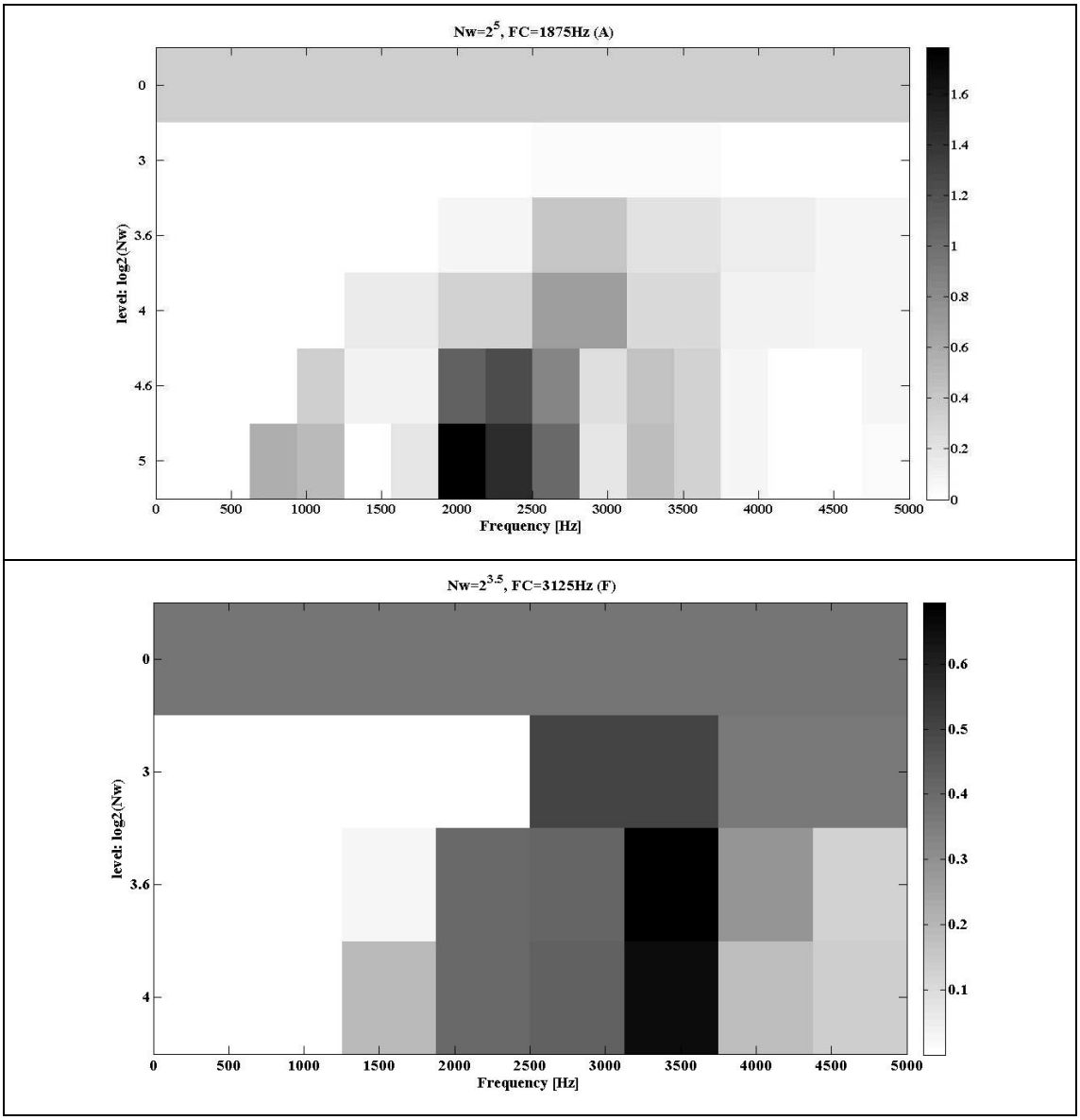

Figure 8 The Kurtogram for Test-1; time intervals 'A' and 'F'

From the SK analysis the centre frequency together with bandwidth for the time intervals A-F were calculated and listed in table 2. In addition, the Kurtosis values associated with the centre frequencies are also presented. The Window size is the

length of data points within that particular window within which the STFT of the signal and corresponding SK values were estimated (equations 1-3). Whilst the centre frequency is the frequency at which the calculated SK value, at that particular windows size, is maximized. It is believed that the higher SNR is achieved at this centre as it matches one of the system natural frequency [12].

Table 2 Estimated features from Kurtogram

	Test 1			*Test 2*		
	Fc(Hz)	**Nw**	**Kurt**	**Fc(Hz)**	**Nw**	**Kurt**
A	1875	32	1.8	1875	32	3.4
B	1875	32	1.7	1875	32	1.7
C	1875	32	3.4	1875	32	1.6
D	625	32	2.4	1875	32	1.9
E	2812	32	3.3	2187	32	3.7
F	3125	11	0.8	2187	32	1.9

Nw: Window size **Kurt**: Kurtosis **Fc**: Centre Frequency

The signals were band- pass filtered at the determined centre frequencies, which were based on the extracted features from the Kurtogram, and resulting time waveforms are presented in figures 9-10[1]. From the figures it was evident that filtered signals offered a higher level of signal to noise ratio showing the capability of SK based filtering for denoising. To quantify the improvements in signal-to-noise Crest factor (CF) values were compared before and after filtering. The CF defined as the ratio of the peak value divided by the signal r.m.s which gives an indication of signal peak-to-average ratio. CF is a traditional method of measuring the smoothness of a signal and therefore a faulty bearing will generate a spiky signal profile resulting an increase in CF .

[1] The Window-based finite impulse response filter was employed for filtering. The size of window used to design the filter was equal to that calculated from the Kurtogram of each signal.

Figure 11, shows the values of CF for filtered and unfiltered signals in which an average increase in CF levels of approximately of 264% and 250 % were noted for Test-1 and Test-2 respectively after bandpass filtering.

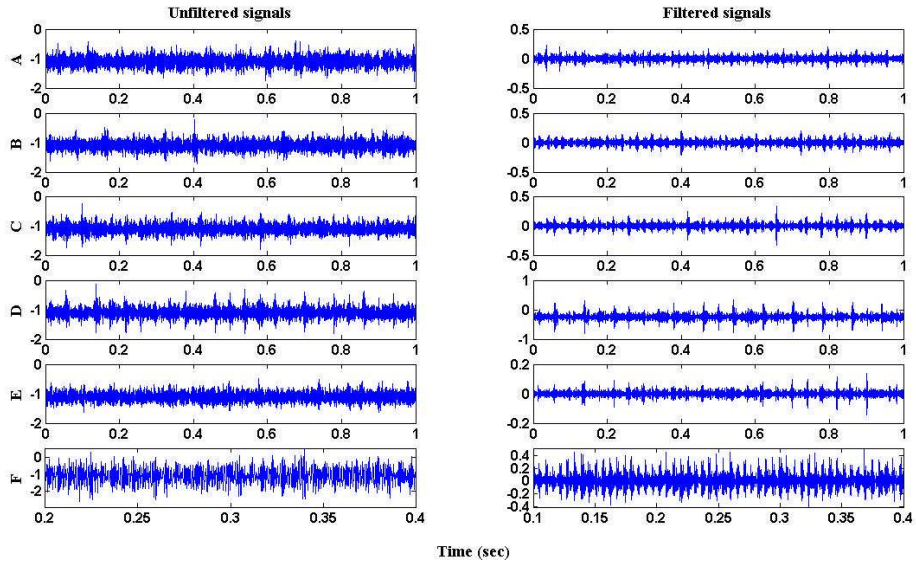

Figure 9 Vibration waveform for test 1 (Filtered designed based on Kurtogram)

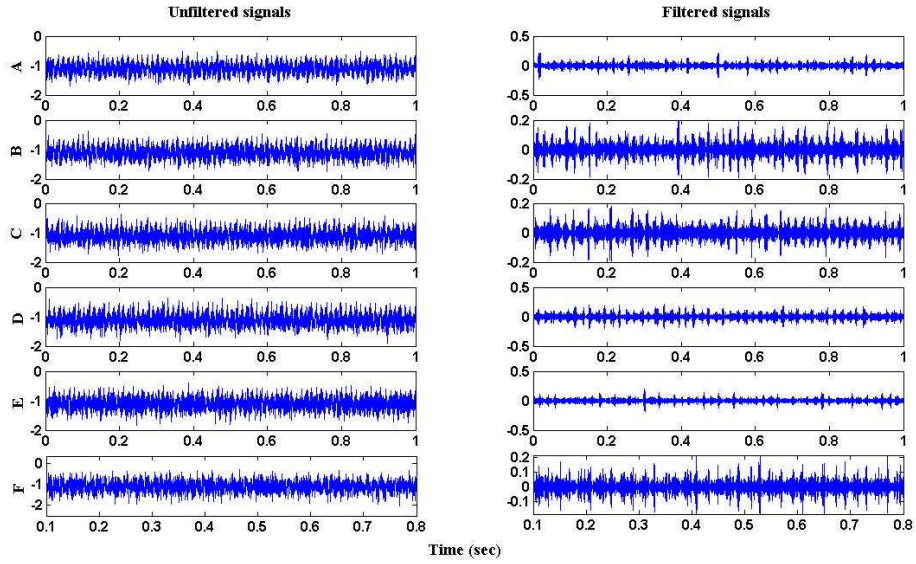

Figure 10 Vibration waveform for test 2 (Filter designed based on Kurtogram)

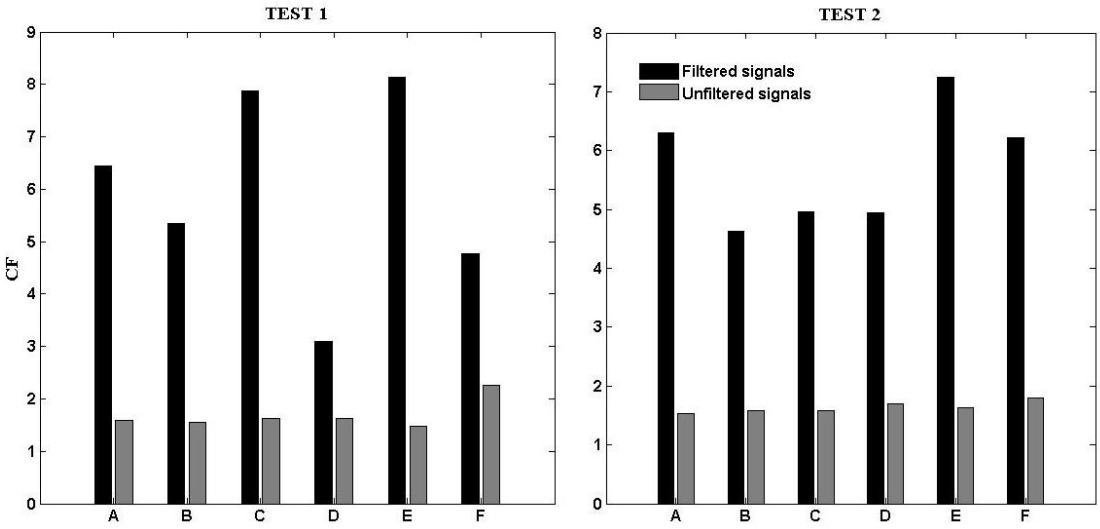

Figure 11 CF values associated with filtered and unfiltered signals

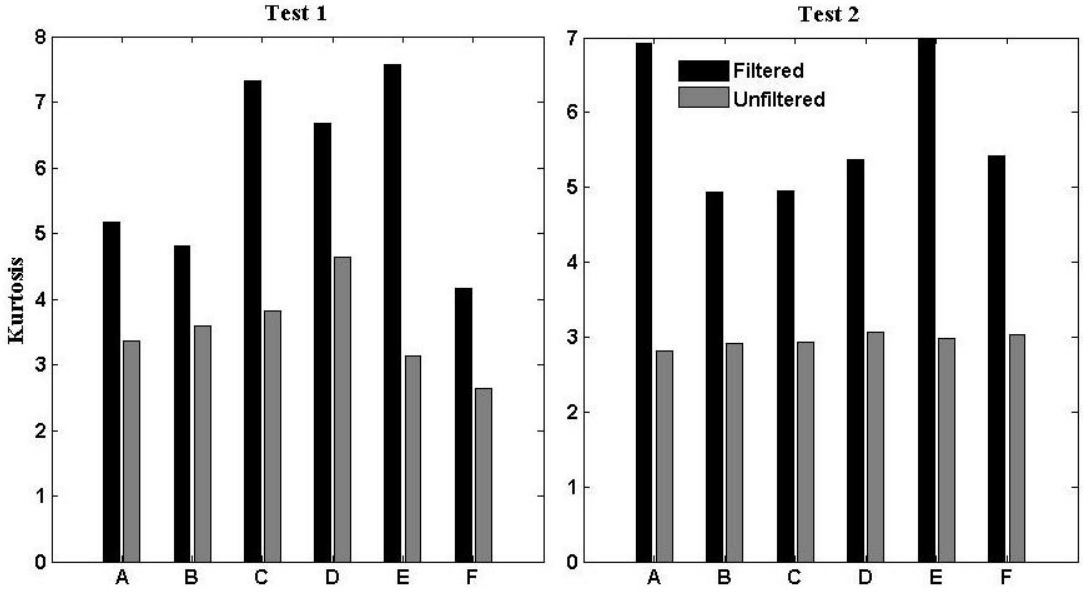

Figure 12 The relative increase in level Kurtosis values after Band-pass filtering

The Kurtosis values of the signals at intervals 'A' to 'F' prior to and after filtering are also presented in figure 12 showing a 70% and 95% average rise in Kurotsis values as a result of band pass filtering for Test-1 and Test-2. This agrees with observation from figures 9 and 10 where the presences of spikes were more evident on the filtered waveforms. The squared envelop of the signals, for both test, were calculated and the corresponding frequency spectrum of the enveloped signals are also presented in figure 13 in which the defect frequency is clearly marked upon the termination of both test. The capability of discriminating the BPF in the corresponding envelop spectrum clearly indicates the effectiveness of SK in diagnosing the fault frequency. In

comparison to the envelop spectrum presented earlier in figure 7 it is evident that the level filtering offered by the Kurtogram had improved earlier detection of the defect frequency, at interval 'D' which is much earlier than noted in figure 7. For Test-2 the SK-based filter did not offer any improvement in earlier detection of the defect frequency suggesting a limitation in its denoising effectiveness.

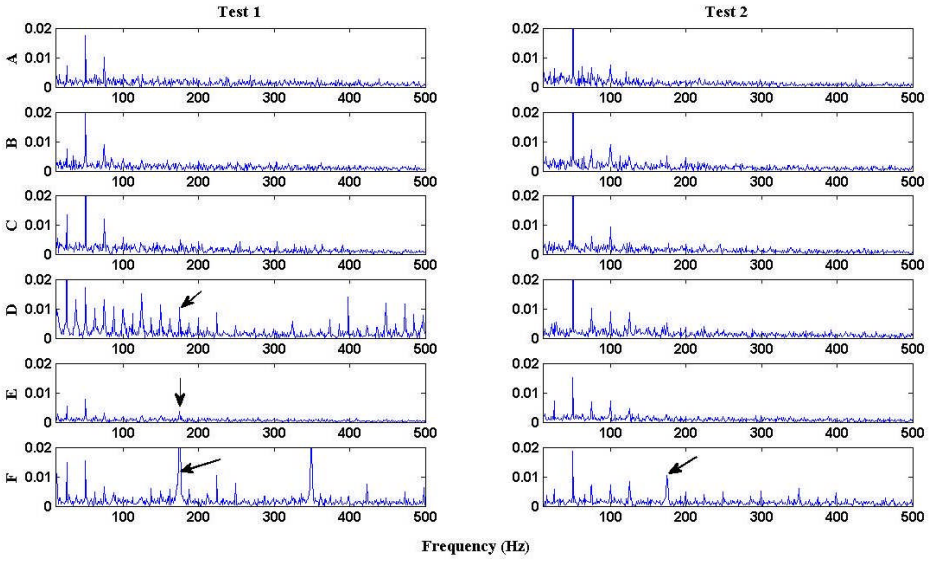

Figure 13 Envelope spectrum of the SK filtered signals

5. Acoustic emission

From figure 2 it was noted an initial increase in AE r.m.s levels between 0-12min for Test-1 and 0-30 min for Test-2. The initial raise in r.m.s values is associated with the run-in stage of the bearings after which the AE activity remained constant for period of 18mins and 2-hrs for first and second tests respectively. For the first test, the level of AE r.m.s started to increase after approximately 1hr into operation suggesting the onset of failure. A similar observation was noted for second test after 3hrs of continuous running. Comparing the overall trend of vibration and AE r.m.s, it is evident that the AE is more sensitive in monitoring the progression of the defect. In addition, AE levels increased approximately one hour before the vibration levels began to change.This was noted in both tests, for instance in test-1 AE levels started to increase at 3hrs of operation whilst vibration levels increased after 4hrs at operation. It must be noted that these are accelerated failure tests and the difference

in period between these techniques (AE and vibration) in identification of the defect will most certainly be much longer for non-accelerated test conditions.

The AE signals for different intervals, as set in table 3, were chosen for further analysis, see figure 14. Interestingly, for Test-1 at time period ‘F’, the AE waveform showed large transient bursts spaced at one of the bearing defect frequencies. This is a classical AE bearing defect phenomenon as noted by several investigators [6, 8, 17]. However, for the second test, the underlying noise level obscures any apparent high transient events in the waveform.

Table 3

	Test 1	**Test 2**
A	35 min	42 min
B	70 min	87 min
C	105 min	132 min
D	140 min	174 min
E	175 min	219 min
F	210 min	267 min

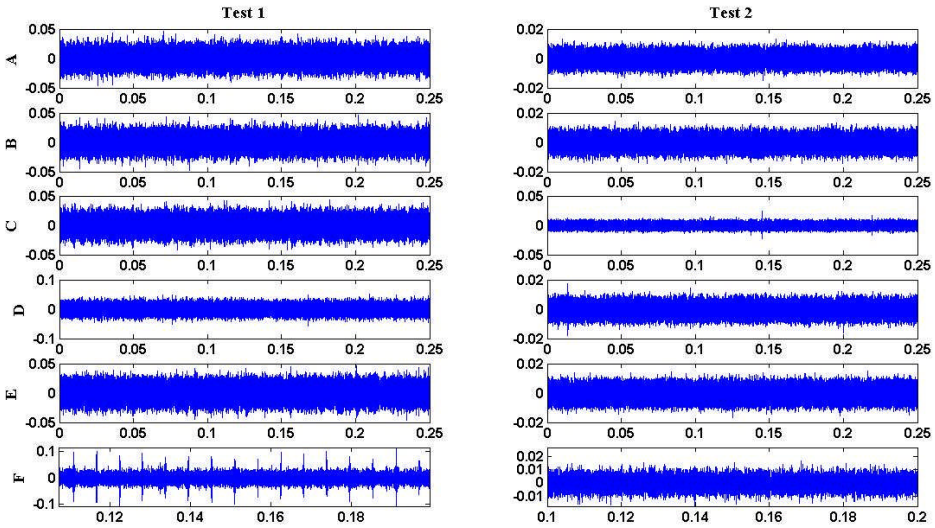

Figure 14 The AE waveform at different time intervals

The frequency spectrum of recorded AE signals show the AE activity is concentrated between 50- 450 kHz, see figure 15. In order to identify any modulating features, the envelop spectrum of the signals were generated using the Hilbert transform. The plots of envelop spectrums for both tests are presented in figure 16. Results from the first test show the presence of the BPF and its harmonics. Surprisingly the presence of the defect frequency 175 Hz, was noted for all the timing intervals (A-F) although the magnitude of the peak increased with time reaching a maximum at the termination of the test . For the second test, the presence of the harmonics noted in the first test were not evident though the second and forth harmonics were noted at the end of the test, time interval 'F'. The reason for inadequate clarity in discriminating of the harmonics and fault frequency is attributed to the presence of noise and therefore a lower signal-to-noise ratio than Test-1.It is worth to mention that, although the two test were quite distinct in the level of SNR; but the observation of the increase on two AE trends in figure 2 and also the harmonics of BPF across the envelop spectrum, upon the termination of the both tests clarifies the effective measurement of AE signals.

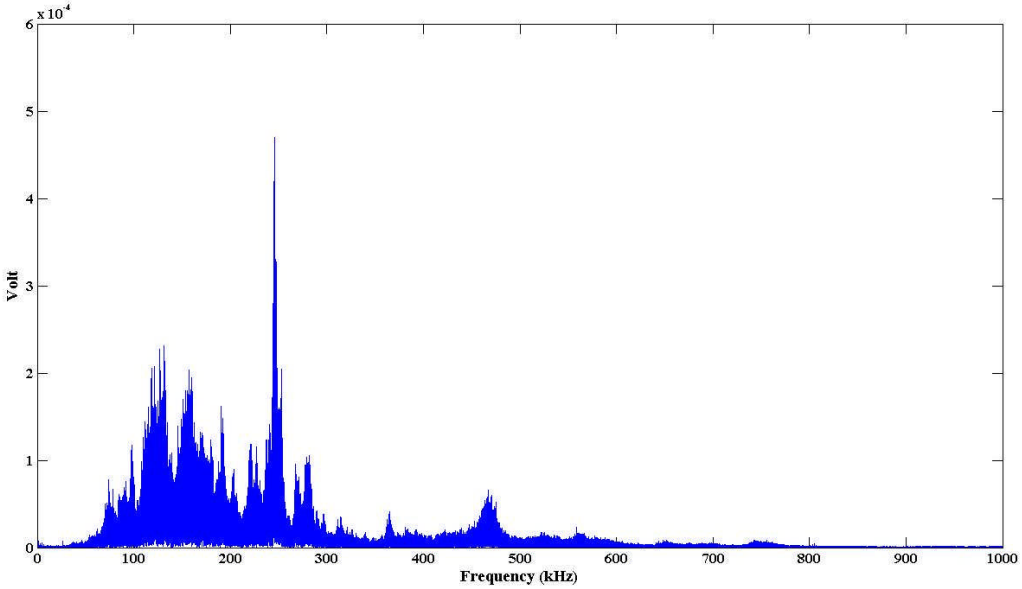

Figure 15 Frequency spectrum of the AE signal

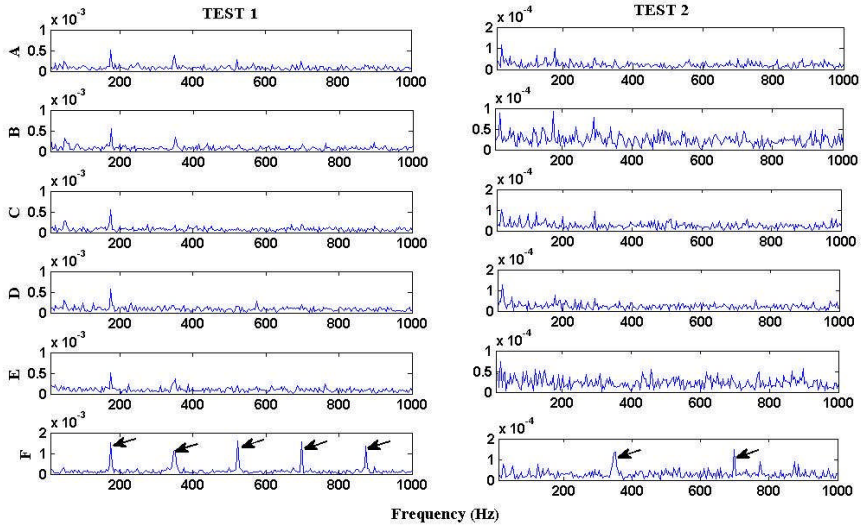

Figure 16 The AE envelop spectrum for the first and second tests

As with the vibration analysis, the SK analysis was undertaken for the AE waveforms. Table 5 shows the optimum frequency bands for time intervals 'A' to 'F'. According to the table, the optimum centre frequencies associated with undamaged race (A-E) were outside the sensor measurement range. This is because for the undamaged bearing the higher frequencies within the sensor measurement range are predominately gaussian so the maximum Kurtosis value occurs at the lower frequency range, below 30 kHz to 40 kHz.

Table 3 Optimum Bandwidth and Centre frequency for AE signal

	Test 1		***Test 2***	
	Fc (Hz)	$\log_2(Nw)$	Fc (Hz)	$\log_2(Nw)$
A	39062	7.5	31250	7
B	31250	7	31250	7.5
C	31250	7	65185	12.5
D	31250	7.5	31250	7.5
E	31250	7.5	15625	8
F	714843	8.5	61523	10.5

The filtered waveforms are presented in figure 17 showing a significant improvement in level of SNR compared with the unfiltered signals in figure 14. This is also manifested in figure 18 in which an average of approximately 242% and 95%

increase in CF values were noted for the filtered signals on Test-1 and Test-2 respectively. Furthermore, figure 19 illustrates the envelope spectrum of the filtered signals based on SK analysis. The BPF and its second harmonic were present across the frequency spectrum for both tests while such observations were not noted for the unfiltered envelope spectrum in figure 16.

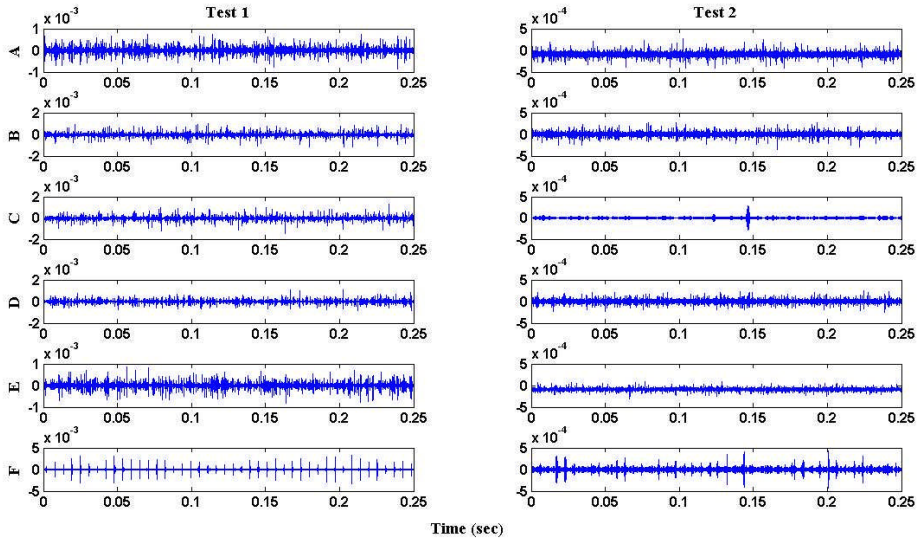

Figure 17 AE waveforms associated with filtered signals

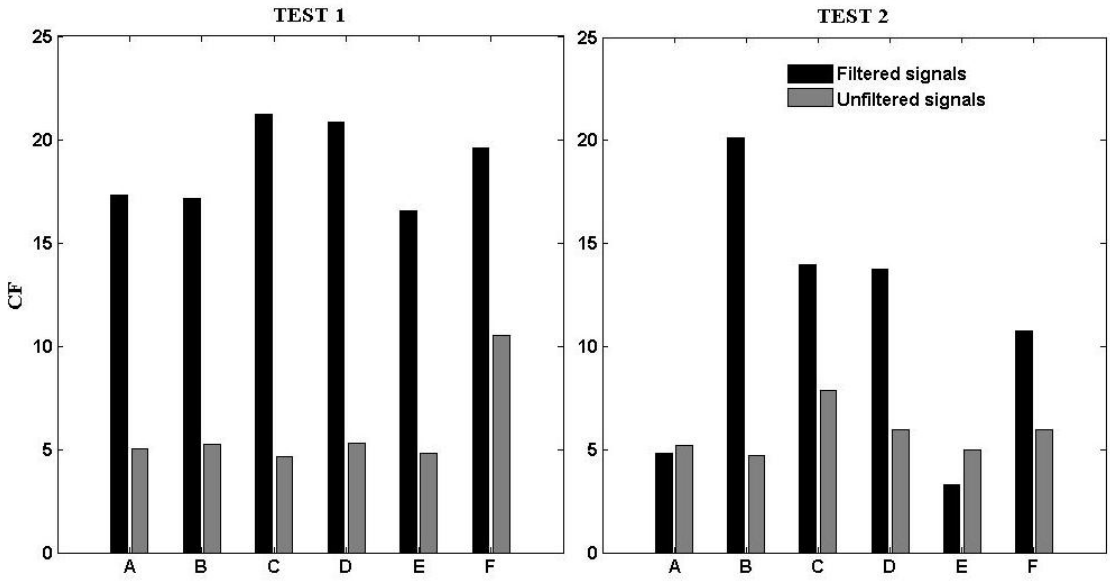

Figure 18 CF values associated with filtered and unfiltered signals

.

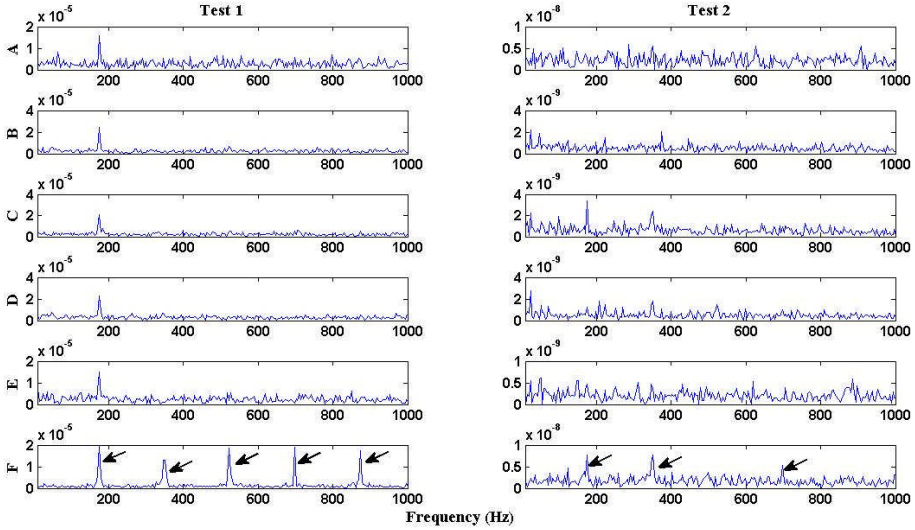

Figure 19 Envelope spectrum of the SK-based filtered signals

Having noted the improvement in signal-to-noise ratio particularly for Test-2, the authors compared the SK to wavelet-based filter analysis. The AE signals were decomposed using Debauches wavelet of order 8 (db8). The reason for choosing db8 as a mother wavelet is firstly because of being orthogonal and secondly the shape of it is close to the mechanical impulse [18]. The envelop spectrum at each level of decomposition (D1-9) were carefully studied and level D1 (500 kHz - 1000 kHz) was found to be the most sensitive for identifying the presence of the defect. The envelop spectrums of the signals at D1 are presented in figure 20 in which BPF and its harmonics are evident upon the termination of both test.

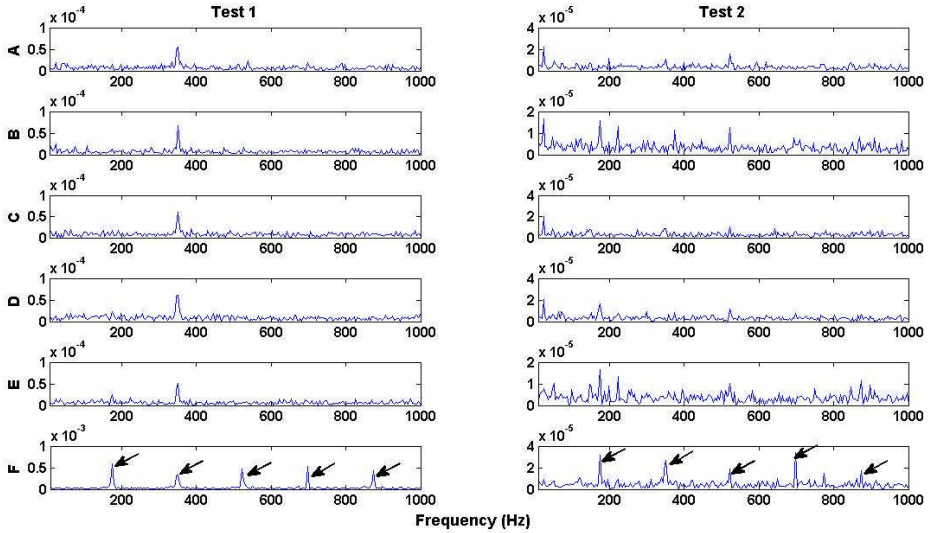

Figure 20 Envelop spectrum of the AE signals at D1

The CF values for the original filtered (SK) and decomposed (db8) signals are presented in figure 21. In comparison to the original values of CF, the SK filtered signals showed an increase in CF of approximately 242% and 95% for Test-1 and Test-2 respectively. Crest factor values noted for decomposed signals (D1) were in the order of 18% and 70% for Test-1 and Test-2 respectively; implying the SK offered the optimum filtered characteristics for identifying impulsive effects, which are typically associated with defective bearings. The waveforms together with CF values at interval 'F' for D1, the original unfiltered waveform and the filtered waveform (SK) are also presented in figure 22 in which the presence of impulsive AE events associated with the defective bearing are most evident for the SK filtered signals. There was only one instance where the wavelet based filter had a better CF than the SK filtered data (Test-1, interval 'F'). This observation reinforced the benefits of applying the SK for defect diagnosis for varying signal-to-noise ratio.

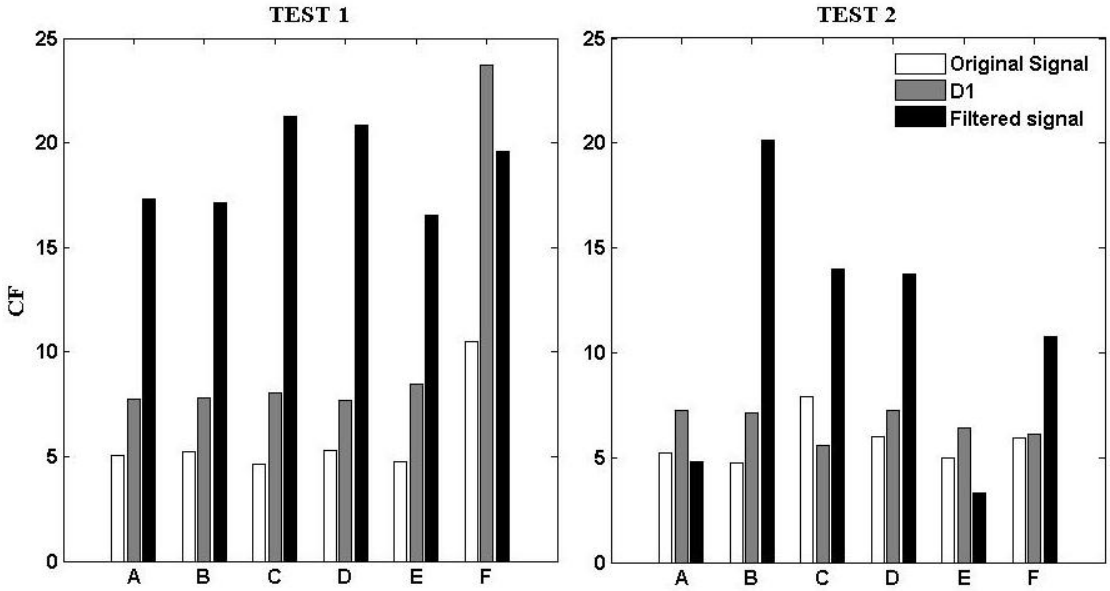

Figure 21 CF value attribute to different diagnostic methods

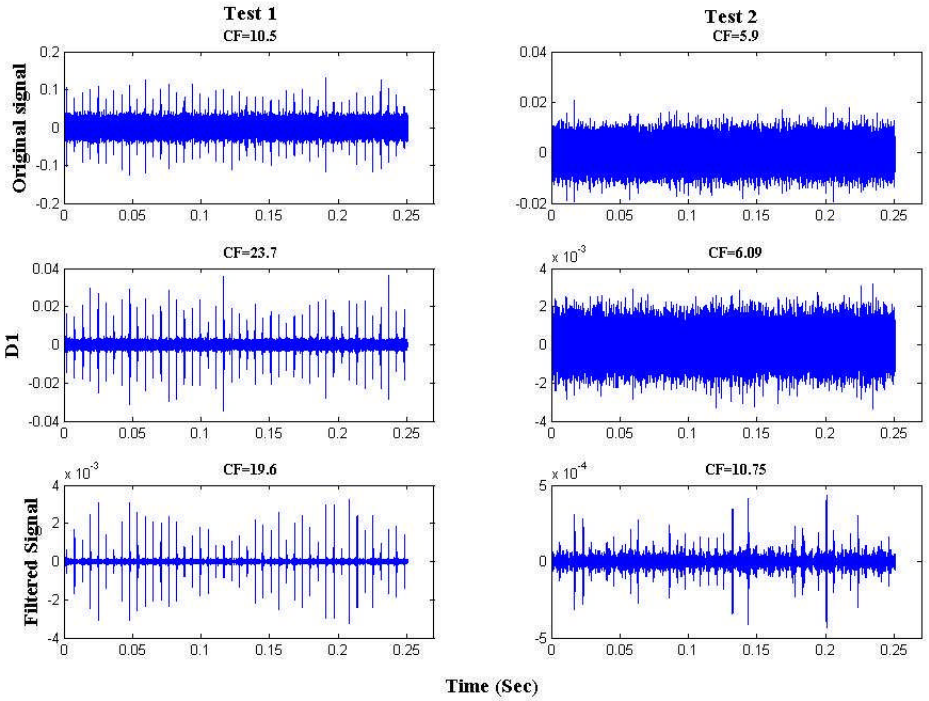

Figure 22 Comparison between D1 and filtered signals at interval 'F'

6. Conclusion

The applicability of both Acoustic Emission and Vibration methods were studied in relation to defect identification of a naturally damaged bearing. From observation it was evident that AE was more sensitive in detecting incipient damage than vibration

reinforcing other investigators [19]. Furthermore, the application of SK analysis and Kurtogram was investigated and it showed the effectiveness in denoising the both AE and vibration signals. The use of the Kurtogram for AE bearing analysis is encouraging and its hoped future researchers explore its full potential.

References

[1] Behzad, M., AlandiHallaj, A., Bastami, A. R., 2009, "Defect Size Estimation in Rolling Element Bearings using Vibration Time Waveform," Insight: Non-Destructive Testing and Condition Monitoring, **51**(8) pp. 426-430.

[2] Patil, M. S., Mathew, J., and Kumar, P. K. R., 2008, "Bearing Signature Analysis as a Medium for Fault Detection: A Review," Journal of Tribology, **130**(1) .

[3] Kar, C., and Mohanty, A. R., 2004, "Application of KS Test in Ball Bearing Fault Diagnosis," Journal of Sound and Vibration, **269**(1-2) pp. 439-454.

[4] Hall, L. D., and Mba, D., 2004, "Acoustic Emissions Diagnosis of Rotor-Stator Rubs using the KS Statistic," Mechanical Systems and Signal Processing, **18**(4) pp. 849-868.

[5] Mba, D., and Rao, R. B. K. N., 2006, "Development of Acoustic Emission Technology for Condition Monitoring and Diagnosis of Rotating Machines: Bearings, Pumps, Gearboxes, Engines, and Rotating Structures," Shock and Vibration Digest, **38**(1) pp. 3-16.

[6] T. Yoshioka, 1992, "Application of Acoustic Emission Technique to Detection of Rolling Bearing Failure," J. Soc. Tribologists Lubrication Eng, **49**.

[7] Elforjani, M., and Mba, D., "Accelerated Natural Fault Diagnosis in Slow Speed Bearings with Acoustic Emission," Engineering Fracture Mechanics, .

[8] Elforjani, M., and Mba, D., 2009, "Assessment of Natural Crack Initiation and its Propagation in Slow Speed Bearings," Nondestructive Testing and Evaluation, **24**(3) pp. 261.

[9] Randall, R. B., 2005, "Applications of Spectral Kurtosis in Machine Diagnostics and Prognostics," Key Engineering Materials, **293-294**pp. 21-30.

[10] Dwyer, R. F., 1983, "A Technique for Improving Detection and Estimation of Signals Contaminated by Under Ice Noise." Journal of the Acoustical Society of America, **74**(1) pp. 124-130.

[11] Antoni, J., 2006, "The Spectral Kurtosis: A Useful Tool for Characterising Non-Stationary Signals," Mechanical Systems and Signal Processing, **20**(2) pp. 282-307.

[12] Antoni, J., and Randall, R. B., 2006, "The Spectral Kurtosis: Application to the Vibratory Surveillance and Diagnostics of Rotating Machines," Mechanical Systems and Signal Processing, **20**(2) pp. 308-331.

[13] Sikorska, J. Z., and Mba, D., 2008, "Challenges and Obstacles in the Application of Acoustic Emission to Process Machinery," Proceedings of the Institution of Mechanical Engineers, Part E: Journal of Process Mechanical Engineering, **222**(1) pp. 1-19.

[14] Zhang, Y., and Randall, R. B., 2009, "Rolling Element Bearing Fault Diagnosis Based on the Combination of Genetic Algorithms and Fast Kurtogram," Mechanical Systems and Signal Processing, **23**(5) pp. 1509-1517.

[15] Jérôme Antoni, http://www.utc.fr/~antoni/ .

[16] Antoni, J., 2007, "Fast Computation of the Kurtogram for the Detection of Transient Faults," Mechanical Systems and Signal Processing, **21**(1) pp. 108-124.

[17] Al-Ghamd, A. M., and Mba, D., 2006, "A Comparative Experimental Study on the use of Acoustic Emission and Vibration Analysis for Bearing Defect Identification and Estimation of Defect Size," Mechanical Systems and Signal Processing, **20**(7) pp. 1537-1571.

[18] Serrano, E. P., and Fabio, M. A., 1996, "Application of the Wavelet Transform to Acoustic Emission Signals Processing," IEEE Transactions on Signal Processing, **44**(5) pp. 1270-1275.

[19] Tan, C. K., Irving, P., and Mba, D., 2007, "A Comparative Experimental Study on the Diagnostic and Prognostic Capabilities of Acoustics Emission, Vibration and Spectrometric Oil Analysis for Spur Gears," Mechanical Systems and Signal Processing, **21**(1) pp. 208-233.

Further reading

[20] Yang, W. X., 2008, "Interpretation of Mechanical Signals using an Improved Hilbert-Huang Transform," Mechanical Systems and Signal Processing, **22**(5) pp. 1061-1071.

[21] Lin, J., and Zuo, M. J., 2003, "Gearbox Fault Diagnosis using Adaptive Wavelet Filter," Mechanical Systems and Signal Processing, **17**(6) pp. 1259-1269.

[22] Altmann, J., and Mathew, J., 2001, "Multiple Band-Pass Autoregressive Demodulation for Rolling-Element Bearing Fault Diagnosis," Mechanical Systems and Signal Processing, **15**(5) pp. 963-977.